

# Large Area ITO-free Flexible White OLEDs with Orgacon™ PEDOT:PSS and Printed Metal Shunting Lines

Stephan Harkema<sup>\*a</sup>, Sibe Mennema<sup>b</sup>, Marco Barink<sup>b</sup>, Harmen Rooms<sup>a</sup>, Joanne S. Wilson<sup>a</sup>, Ton van Mol<sup>a</sup> and Dirk Bollen<sup>c</sup>

<sup>a</sup>Holst Centre TNO, High Tech Campus 31, 5656 AE Eindhoven, The Netherlands

<sup>b</sup>TNO Science and Industry, de Rondom 1, 5612 AP Eindhoven, The Netherlands

<sup>c</sup>Agfa Gevaert B.V., Septestraat 27, B-2640 Mortsel, Belgium

## ABSTRACT

We demonstrate the feasibility of white organic light-emitting diodes that exclude the transparent conductor indium-tin-oxide. Instead, a highly conductive Orgacon™ PEDOT:PSS material in combination with a metal support structure is used as transparent anode and hole-injection layer. The PEDOT:PSS exhibits a conductivity of  $460 \pm 20$  S/cm and a work function of  $5.35 \pm 0.05$  eV. On ITO-free OLEDs on glass with an active area of  $\sim 6$  cm<sup>2</sup> the inclusion of 120 nm thick printed metal lines reduces the variation in brightness from 35% to 20%. The ITO-free concept based on PEDOT:PSS with printed metal structures is scaled up to large flexible OLEDs with a size of 150 cm<sup>2</sup> on a heat-stabilized Teonex® Polyethylene Naphtalate foil. The voltage distribution across the various electrodes was verified by a finite element model, allowing a prediction of the OLED brightness and homogeneity over large areas.

**Keywords:** OLED, white-emitting, flexible, ORGACON PEDOT:PSS, ITO-free, metal grid, printed silver

## 1. INTRODUCTION

In organic light-emitting diodes (OLEDs) at least one of the electrodes should be both transparent and electrically conductive. The most common choice for this transparent conductor has been indium-tin-oxide (ITO)<sup>1</sup>. However, with a growing demand towards roll-to-roll production of large area (flexible) OLEDs for lighting applications the usage of ITO is a major concern towards the commercialization of OLED technology. In particular, the costs of material<sup>2</sup>, deposition and patterning of ITO as well as the limited world supply of indium are major obstacles for highly cost-effective production. The brittleness of ITO is an additional problem that leads to mechanical instability of roll-to-roll processed flexible devices.

Another important issue is the relatively limited conductivity of ITO. For lighting applications, the surface area of OLEDs is expected to be in the order of several hundreds cm<sup>2</sup>. OLEDs with an active area of this size require a sheet resistance of the transparent anode that is on par with the conductivity of the cathode, in the order of 105 S/cm or better. Only with such low resistances Ohmic losses and associated non-uniformity of the light emission can be avoided. However, when ITO is deposited on flexible plastic substrates, such as polyethylene naphtalate (PEN) and polyethylene terephthalate (PET), the annealing temperature is limited by the glass transition temperature of the substrate. Due to the lower annealing temperature the conductivity of an ITO layer on PEN or PET with a typical layer thickness of 100 nm can only reach  $5\text{-}7 \cdot 10^3$  S/cm ( $15\text{-}20$  Ω/square). For large surface area OLEDs as used for lighting applications a metallic support structure is thus necessary to achieve the required conductivity. For esthetical reasons, it is desirable to have a relatively fine mesh metallic support structure. Such a fine mesh metallic support structure subsequently lowers the sheet resistivity requirements for the anode of the device. Consequently, the choice of anode material is no longer restricted to ITO. Here we demonstrate ITO-free, flexible, white-emitting, polymer-based OLEDs with a low cost, solution-processable single layer of poly(3,4-ethylenedioxythiophene):poly(styrenesulphonic acid) (PEDOT:PSS), that acts as both the anode and hole injection layer.

\* stephan.harkema@tno.nl; phone +31 (0) 40 277 4047; fax +31 (0) 40 274 6400; holstcentre.com

Printed metallic structures that improve the anode conductivity are combined with this PEDOT:PSS layer for scaling up to large areas. Both the metallic support structure and the PEDOT:PSS can be deposited and cured in air. The PEDOT:PSS formulation was optimized for processability, in-plane conductivity and efficient hole injection into a white-emitting polymer. The voltage drop across a series of ITO-free anodes is analyzed with finite element calculations and is compared with the measured homogeneity of light emission. The technology is scaled up to flexible 150 cm<sup>2</sup> devices on PET and PEN foils, and the performance of these large area ITO-free devices with a thin film barrier is compared to equivalent glass-based devices containing ITO.

## 2. DEVICE STRUCTURE AND MATERIALS

### 2.1 Glass-based organic light-emitting diodes

The OLED architecture consists of PEDOT:PSS and a light-emitting polymer (Merck Livlux™) on top of either an ITO or an insulating substrate. In the latter case the hole-injection layer PEDOT:PSS (Agfa Orgacon™) serves as transparent anode. The PEDOT:PSS and the light-emitting polymer (Merck Livlux™) were deposited from solution by spin-coating under ambient conditions. Typical layer thicknesses were 100 nm for PEDOT:PSS and 80 nm for light-emitting polymer (LEP). The cathode contains thin barium (5 nm) and aluminum (100 nm).

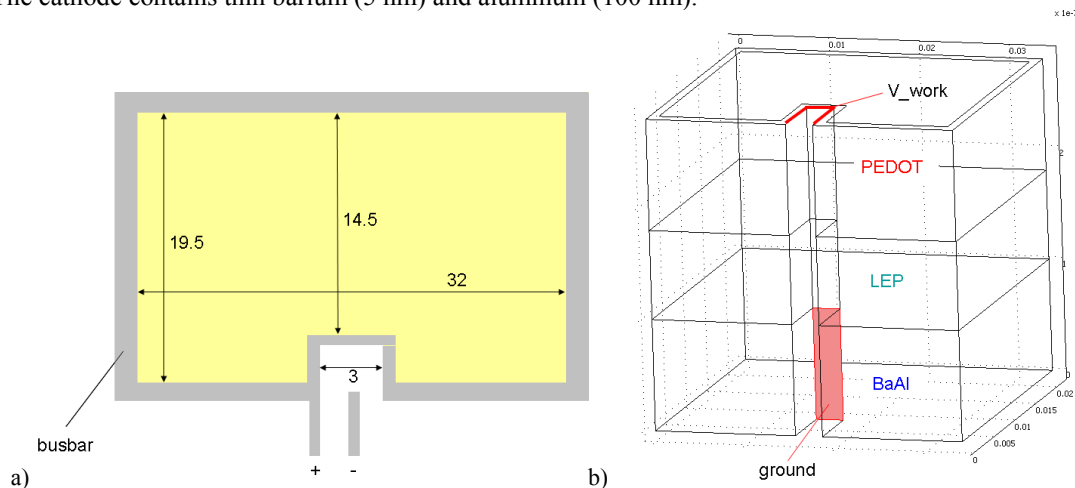


Fig. 1. a) Top view of a 5.75 cm<sup>2</sup> glass-based OLED. b) 3D representation of the active layers in an ITO-free OLED. The PEDOT:PSS layer serves here as transparent anode and hole-injection layer. The vertical scale is exaggerated to enhance visibility.

The current-voltage-light (IVL) characteristics of the OLED devices were measured using a Keithley Model 2400 general-purpose sourcemeter. During the IVL cycle, the brightness was monitored by a photodiode that was calibrated with a Konica Minolta LS-100 luminance meter. The luminance meter was mounted orthogonally to the OLED that was connected to a Keithley Model 6517A electrometer/high-resistance meter.

### 2.2 Orgacon™ PEDOT

For ITO-free OLEDs, a high-conducting hole-injection layer ORGACON™ PEDOT:PSS was developed. The PEDOT:PSS morphology, which is characterized by PEDOT-rich particles with an insulating PSS-rich shell<sup>3</sup>, was enhanced by selecting appropriate additives and adapted synthetic routes to achieve a high-conducting formulations with a high work function. Clevios P VP AI 4083 and Clevios PH500 were used as reference materials.

The work function of PEDOT:PSS thin films was characterized using a KP Technology Scanning Kelvin Probe Microscope. The work function resolution of the Kelvin Probe is 1 – 10 meV. The Kelvin Probe tip is set up in a shielded chamber, which was flushed with nitrogen to minimize water up-take by the hygroscopic PEDOT:PSS. Reported values for the work function are averages of a scan over a distance of several cm and values for the standard deviation are associated with spatial variation of the work function. Absolute values for the work function were

calculated using Highly Oriented Pyrolytic Graphite as reference with a work function of 4475 meV<sup>4</sup>. In addition to HOPG, commercial PEDOT:PSS formulations were measured for benchmarking purposes. The high conductive variant PH500 was prepared according to instructions provided by the material supplier.

The conductivity of spin-coated PEDOT:PSS was determined through 4-points resistance measurements. Gold contacts were evaporated on top of the PEDOT:PSS and these were contacted by a Keithley 2400 source meter. The thickness of the films was determined using a Veeco DEKTAK D6 profilometer.

Table 1: Work functions, conductivities and layer thicknesses of thin PEDOT:PSS films

<b>PEDOT:PSS formulation</b>	<b>work function (eV)</b>	<b><math>\sigma</math> (S/cm)</b>	<b>h (nm)</b>
Clevios P VP AI 4083	5.19±0.05	(3.2±0.5)·10 <sup>-4</sup>	84±3
Clevios PH500 with 5 % DMSO	5.23±0.05	(4.1±0.1)·10 <sup>2</sup>	81±2
Orgacon™	5.37±0.05	(4.6±0.2)·10 <sup>2</sup>	79±2

### 3. ANODE

#### 3.1 Requirements

To achieve a homogeneous light-output from a large area lighting tile, the applied current needs to be distributed by both the metal grid and by the organic anode material. While the former enhances the brightness homogeneity over the entire active area of the lighting tile, the conduction of the latter determines the local brightness homogeneity within a segment that is defined by the metal mesh. The dimensions of the metal grid that supports a PEDOT:PSS anode are defined by the desired anode sheet resistance, the metal grid spacing and the allowed non-emitting (or “dead”) area. The limitation here is the allowed local brightness variation. At the time of writing, we aim for a 20 % local and overall brightness variation, at most a non-emitting area of 10% and an anode sheet resistance of 1  $\Omega$ . Based on the measured conductivity of the PEDOT:PSS hole injection layer (as given in Table 1), the required metal grid spacing to achieve these aims was calculated.

#### 3.2 Metal support structure

A commercial nano-particle ink, Cabot AG-IJ-G-100-S1, was inkjet printed onto the glass substrate by a Fuji Film Dimatix Materials Printer (DMP 2381) with 10 pl drop size print-heads in a clean room environment. The printed metal lines were sintered in a temperature controlled oven for 30 minutes at 150°C. Single line printing gave 120 nm thick lines with a resistivity that is roughly 20 times that of bulk silver.

Table 2. Details of the printed shunting lines.

	Parameter	Remark
Type of ink	AG-IJ-G-100-S1	Cabot Ag nano-particle ink
Line width	200 $\mu\text{m}$	
Height	120 nm	Average height
Sheet resistance	$\sim 20 \times \rho_{\text{Ag,bulk}}$	

## 4. RESULTS AND DISCUSSION

### 4.1 White OLEDs on glass

Omitting the ITO from the OLED requires a high conductive hole-injection layer to allow light to be emitted from the center of the OLED. This is exemplified by OLEDs incorporating PEDOT:PSS formulations with different conductivities, shown in Fig. 2. In the left OLED a commercial low-conductive PEDOT:PSS was used that has a conductivity of  $3.2 \cdot 10^{-4}$  S/cm. Without the ITO layer, the conductivity of the anode was insufficient and as a result only the edge of the device emitted light. In the middle device, an Orgacon™ PEDOT:PSS with a conductivity of  $2.1 \cdot 10^{-4}$  S/cm serves as transparent anode. The increase in sheet resistance of this organic anode with respect to ITO leads to a voltage drop towards the center of the device and subsequently a lower brightness. The middle OLED has a visible brightness drop from edge to center that was measured to be as high as 50 %. For the right device, with a more conductive PEDOT:PSS formulation, the drop was measured to be  $\sim 30$  %.

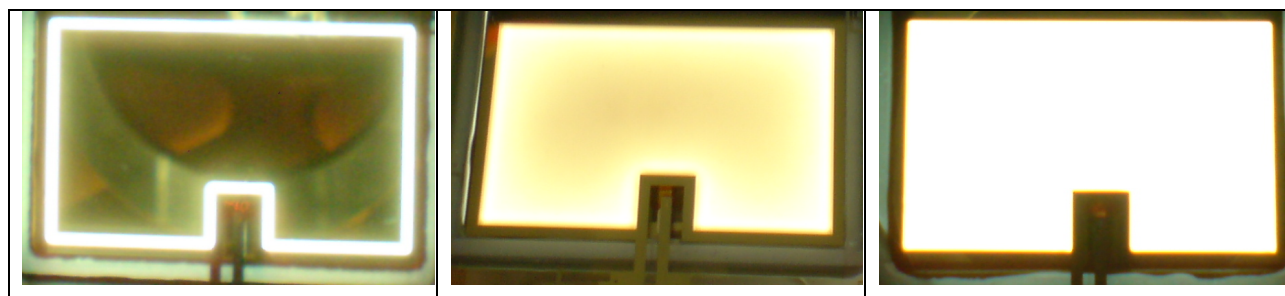


Fig. 2.  $5.75 \text{ cm}^2$  glass-based ITO-free OLED with a PEDOT:PSS hole-injection layer with, from left to right, increasing conductivity. All images were taken at the same applied current density.

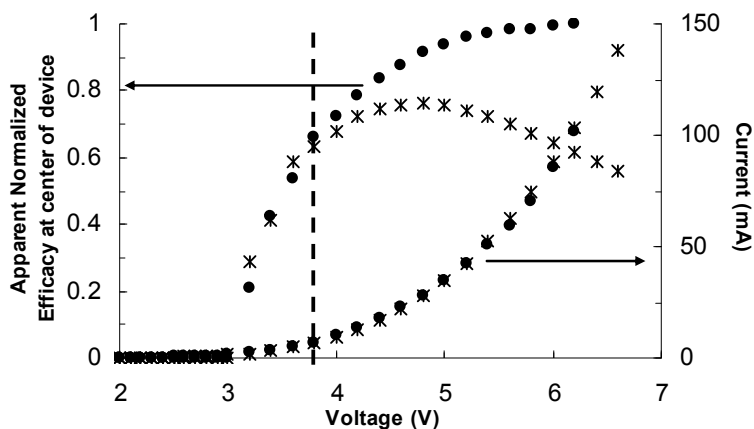


Fig. 3. IVL scan of a 5.75 cm<sup>2</sup> glass-based ITO-free OLED with an high-conductive PEDOT:PSS (460 S/cm) hole-injection layer (crosses) and a reference device with an ITO and a low conductive PEDOT:PSS hole-injection layer as the anode (circles).

In Fig. 3, the apparent normalized current efficiency at the center of the OLED versus voltage and current versus voltage are given for two samples, namely a sample with ITO and low conducting PEDOT as anode and a sample with a high conductive PEDOT as anode. The current efficiency was calculated with the brightness at the center of the device where the voltage drop of the anode of the ITO-free device resulted in a lower brightness. The current and current efficiency graphs overlap up to ~3.8 V, above which the current efficiency dropped for the device without ITO. At an applied voltage of 5.7 V the edge to center brightness difference was ~30 %.

A finite element based simulation model was used to calculate the anode voltage distribution and the brightness variation associated to the voltage drop. The approach of the model is described in detail in ref. 5 and the properties of the layers are given in Table 3. The model was adapted to include the impact of metal lines on the ITO-free devices (Fig. 2) and we focus here in particularly on the application of printed metal lines.

Table 3. Conduction values used for finite element modeling

Component	Parameter	Remark
Cathode	t: 100 nm $\sigma$ : $3.55 \times 10^5$ S/cm	Considered as a single layer of pure Al
LEP	t: 80 nm $\sigma$ : obtained from IVL	Merck Livilux™
PEDOT:PSS	t: 100 nm $\sigma$ : $4.6 \times 10^2$ S/cm	Agfa Orgacon™
ITO	t: 130 nm $\sigma$ : $3.85 \times 10^3$ S/cm	20 $\Omega$ /square
Al busbar	w: 1 mm t: 1.5 $\mu$ m $\sigma$ : $3.55 \times 10^5$ S/cm	

With the parameters listed in Table 3, the voltage and brightness drop for an ITO-free OLED were calculated as a function of applied voltage to improve the understanding of the behavior observed in the IVL graph (Fig. 3). At a voltage of 3.75 V, the voltage drop was very small (0.05 V) and the brightness variation over the 5.75 cm<sup>2</sup> was calculated to be 5 cd/m<sup>2</sup>. At 4.1 V, the calculated values for voltage drop and brightness increased to 0.08 V and 14 cd/m<sup>2</sup>. Applying a higher voltage increases the voltage drop and brightness inhomogeneity. Our calculations were done up to 5.7 V at which the voltage drop was 0.43 V and the brightness inhomogeneity was 35%. The inhomogeneity of a device without metal support structure, as shown in 4a, was measured to be on average 35.0 ± 2.5 %. The outcome of our calculations was compared to a model approach recent published by K. Neyts *et al.*<sup>6</sup>. Calculations based on both approaches gave a voltage that dropped by slightly more than 0.4 V.

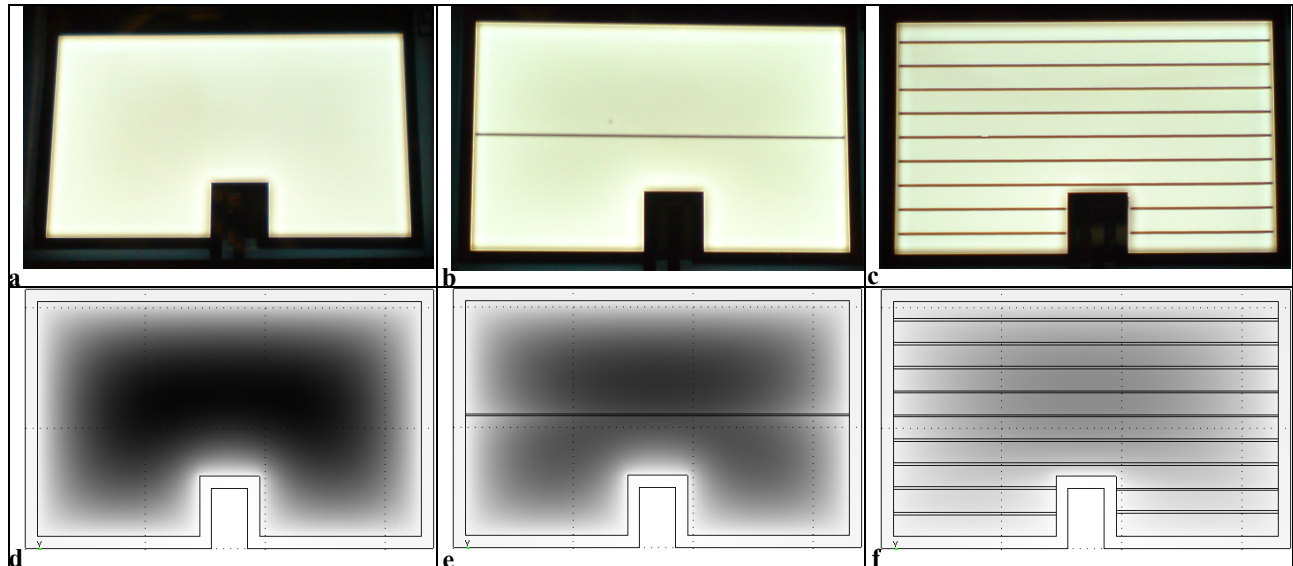


Fig. 4. 5.75 cm<sup>2</sup> glass-based ITO-free OLED with a high conducting PEDOT:PSS hole-injection layer (460 S/cm) and with a) no metal support structures, b) a single printed Ag metal line and c) a series of metal lines with a periodicity of 1 line per 2 mm and a width of 200 μm. All images were taken at the same applied current density. e) Calculated distribution of voltage and brightness of a 5.75 cm<sup>2</sup> glass-based ITO-free OLED without and e,f) with printed shunting lines at a voltage of 5.7 V. The brightness range is static for all three images and is presented in a range from dark (35 % loss in brightness) to bright (no loss in brightness). The maximum variation in brightness was calculated to be at most 35 % (d), 30 % (e) and 16 % (f).

A single silver line with an average height of 120 nm and width of ~200 μm was inkjet printed onto the glass substrate prior to the deposition of PEDOT:PSS. After sintering, the printed silver has a resistivity that is 20 times higher than the bulk resistivity of silver. Based on calculations of the current distribution a very modest improvement of 5 % to yield a 30 % brightness variation over the device is expected at 5.7 V (4e). Increasing the number of printed silver lines from 1 to 9 with a periodicity of 1 line per 2 mm (10 % area coverage) reduced the inhomogeneity in brightness further to 16 % (4f). Brightness measurements of the devices shown in 4 gave 32 %, 26 % and 20 % brightness drop across the device. The current-voltage curves of the OLEDs with shunting lines (not shown here) were nearly identical to the device without any printed silver lines, which indicates that the presence of these lines does not affect the electrical performance.

The OLEDs shown in Fig. 2 and Fig. 4 demonstrate the feasibility of an ITO-free anode based on PEDOT:PSS with a metal support structure, as opposed to thermal evaporation or sputtering in combination with photolithography. Increasing the conductivity, dimensions and spacing between the printed metal structures enable further improvement of the device homogeneity and allow scalability of the concept.

## 4.2 Flexible white OLEDs with a metal grid support PEDOT:PSS anode

Flexible lighting tiles with a surface area of  $\sim 150 \text{ cm}^2$  have been manufactured on heat-stabilized Teonex® Polyethylene Naphtalate (PEN, Dupont Teijin Films). The transparent barrier on foil was based on low-temperature plasma deposited amorphous hydrogenated silicon nitride ( $a\text{-SiN}_x\text{:H}$ ) films as the intrinsic moisture barrier and was stacked with planarization layers to spatially separate defects in these films<sup>7</sup>. To limit the ingress of water and oxygen, the before named moisture barrier was also applied as encapsulation stack on top of the OLED element that was made with the same organic materials as the glass-based devices. Devices without ITO were obtained by omitting the deposition and subsequent post-processing thereof. This eliminated approximately a dozen processing steps. Printing of metal lines was accomplished with inkjet printing and screen printing of different micro- and nano-particle inks (see for instance ref. [8]). IVL analysis (not shown here) of the devices showed a comparable electrical performance with an initial current efficiency that is in agreement to the glass-based devices and the data provided by the material supplier. Finite element modeling verified that the brightness variation was below the set specification of 20 %.

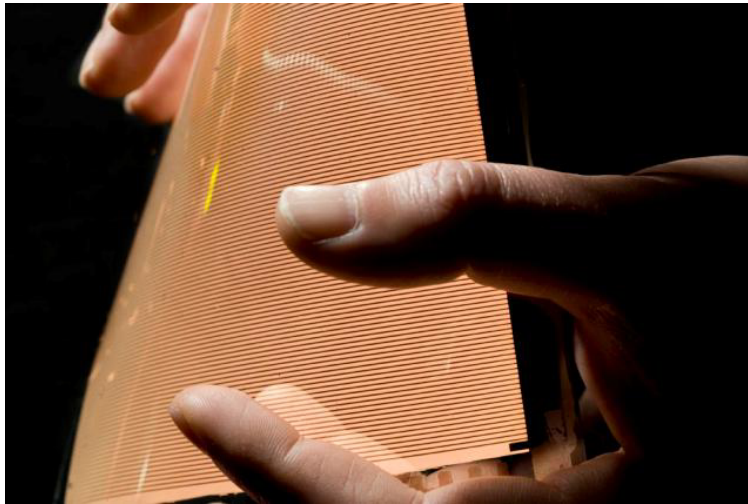


Fig. 5. Flexible ITO-free white OLEDs on Teonex® PEN foil (provided by Dupont Teijin Films) with a printed metal line structure that supports the Orgacon™ high-conductive PEDOT:PSS anode.

## 5. CONCLUSIONS

The classical layer stacking of an OLED includes ITO as the transparent anode material. Increasing the size of the OLED to hundreds of square centimeters requires a lower sheet resistance than ITO enables. The reduction of the anode sheet resistance requires the application of metal, whether or not the classical OLED stack is maintained. Our approach has been to develop a high conducting Orgacon™ PEDOT:PSS with a conductivity of  $460 \pm 20 \text{ S/cm}$ , that serves as transparent anode and facilitates hole-injection into the emitting material, and to combine this organic material with a metal support structure. Device studies and modeling have demonstrated the feasibility of printed metal shunting lines in OLEDs with an active area of several  $\text{cm}^2$ . We have further demonstrated that scaling of this approach to a size of nearly  $150 \text{ cm}^2$  is compatible with low temperature processing on heat-stabilized Teonex® Polyethylene Naphtalate, and does not compromise the electrical performance of the OLED.

## ACKNOWLEDGEMENTS

The Holst Centre is an open innovation research centre founded by TNO and IMEC that is developing roll-to-roll production techniques for foil-based organic electronics and wireless autonomous transducer solutions, in cooperation with industry and universities. The authors would like to acknowledge and thank the European Commission for the financial support via ICT-2007.3.2/216641 Fast2Light Project. This research has further been funded by the Dutch

Ministry of Economic Affairs, Philips Research, Dupont Teijin Films and Agfa Gevaert. Merck KGaA is gratefully acknowledged for providing the white light-emitting polymer.

The experimental work has been performed in the Philips Miplaza research facilities. Manufacturing of OLEDs has been performed in the pre-pilot line of the Device Process Facilities, with thanks to Leo Toonen, Peter Rensing, Walter Stals, Eric Rubingh and Gerwin Kirchner. Adri van der Waal (TNO Science and Industry) is acknowledged for the application of the finite element model. The authors also gratefully acknowledge Edward Young, Mary Kilitziraki, Ferdie van Assche, Margreet de Kok and Paul Blom (Holst Centre) for support and fruitful discussions.

## REFERENCES

- [1] Tang C.W., and VanSlyke S.A., "Organic electroluminescent diodes" *Appl. Phys. Lett.* 51, p. 913 (1987)
- [2] USGS Annual Publications, USGS website (<http://minerals.usgs.gov/minerals/pubs/commodity/indium/>)
- [3] De Kok, M.M., Buechel, M., Vulto, S.I.E., Van de Weijer, P., Meulen Kamp, E.A., De Winter, S.H.P.M., Mank, A.J.G., Vorstenbosch, H.J.M., Weijtens C.H.L. and Van Elsbergen, V., "Modification of PEDOT:PSS as hole injection layer in polymer LEDs", *Phys. Stat. Sol. (a)* 201, p. 1342 (2004)
- [4] Hansen W.N., and Hansen, G.J., "Standard reference surfaces for work function measurements in air", *Surf. Sci.* 481, p. 172 (2001)
- [5] Gielen, A.W.J., Barink, M., Van den Brand, J. and Van Mol, A.M.B., "The electro-thermal-mechanical performance of an OLED: A multi-physics model study" *Proc. EuroSimE*, p. 1 (2009)
- [6] Neyts, K., Real, A., Marescaux, M., Mladenovski, S. and Beeckman, J., "Conductor grid optimization for luminance loss reduction in organic light emitting diodes", *J. Appl. Phys.* 103, p. 093113/1 (2008)
- [7] Van Assche, F.J.H., Rooms, H.C.A., Young, E., Michels, J., Van Mol, A.M.B., Rietjens, G., Van de Weijer, P., Bouten, P., "Thin-film barrier on foil for organic LED lamps", *Proc. AIMCAL* (2008)
- [8] Rubingh, E.J., Kruijt P. and Andriessen R., "Towards TCO-less large area OLEDs for lighting applications", *Proc. LOPE-C* (2009)